HHS Public Access

Author manuscript

J Am Chem Soc. Author manuscript; available in PMC 2017 October 13.

Published in final edited form as:

J Am Chem Soc. 2017 September 20; 139(37): 13193–13199. doi:10.1021/jacs.7b07656.

Effect of Redox Partner Binding on Cytochrome P450 Conformational Dynamics

Dipanwita Batabyal, **Logan S. Richards**, and **Thomas L. Poulos***

Departments of Molecular Biology and Biochemistry, Pharmaceutical Sciences, and Chemistry, University of California, Irvine, California 92697-3900, United States

Abstract

Previous crystal structures of cytochrome P450cam complexed with its redox partner, putidaredoxin (Pdx), shows that P450cam adopts the open conformation. It has been hypothesized that the Pdx-induced shift toward the open state frees the essential Asp251 from salt bridges with Arg186 and Lys178 so that Asp251 can participate in a proton relay network required for O_2 activation. This in part explains why P450cam has such a strict requirement for Pdx. One problem with this view is that looser substrate-protein interactions in the open state may not be compatible with the observed regio- and stereoselective hydroxylation. In the present study, molecular dynamics simulations show that Pdx binding favors a conformation that stabilizes the active site and decreases camphor mobility yet retains a partially open conformation compatible with the required proton relay network. The R186A mutant which frees Asp251 in the absence of Pdx retains good enzyme activity, and the crystal structure shows that product, 5-*exo*-hydroxycamphor, is bound. This indicates that rupture of the Asp251-Arg186 relaxes selectivity with respect to source of electrons and enables X-ray generated reducing equivalents to support substrate hydroxylation. These combined computational and experimental results are consistent with the proposed role of Pdx in assisting the release of Asp251 from ion pairs so that it can participate in proton-coupled electron transfer.

Graphical Abstract

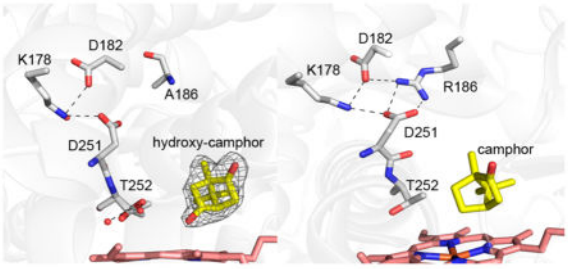

*Corresponding Author: poulos@uci.edu.

ORCID

Thomas L. Poulos: 0000-0002-5648-3510

The authors declare no competing financial interest.

Supporting Information

The Supporting Information is available free of charge on the ACS Publications website at DOI: 10.1021/jacs.7b07656.

Figures S1–S4 (PDF)

INTRODUCTION

Cytochromes P450 are best known for catalyzing mono-oxygenation reactions, wherein a single O_2-derived oxygen atom is inserted into an unactivated C-H bond. Being one of Nature's largest enzyme families, P450s often are found wherever oxidation reactions are required for the biosynthesis of important biomolecules or in the detoxification of various xenobiotics. Although there is a bewilderingly large number of P450s, they all share a common catalytic cycle (Figure 1).

This cycle requires two electron transfer steps, wherein NAD(P)H reducing equivalents are delivered to the P450 heme via a flavin or iron-sulfur protein redox partner. Many P450s are promiscuous with respect to redox partner, and very often catalysis can be supported by non-native redox partners. An important exception is P450cam, the camphor mono-oxygenase from *Pseudomonas putida*. With P450cam, the first electron transfer step (2 in Figure 1) can be supported by various low potential reductants, but the second step (3 in Figure 1) requires the *P. putida* Fe_2S_2 ferredoxin, putidaredoxin (Pdx).[1] It has long been postulated that Pdx must play some type of effector role in addition to serving as a source of electrons. P450cam-Pdx crystal structures[2,3] showed that the binding of Pdx favors the so-called open form of P450cam (Figure 2).

That Pdx favors binding to the open P450cam conformer is well supported by spectroscopic[4,5] and direct binding assays.[6] These long-range effects of Pdx binding on P450cam structural dynamics were first documented in pioneering NMR studies.[7] These results raise the possibility that the second electron transfer step resulting in O-O bond cleavage requires P450cam to adopt the open conformer. A structural basis for this possibility has led to the "Asp switch hypothesis", wherein Pdx binding promotes a structural change that triggers formation of the proton relay network involving Asp251.[3] We know Asp251 is essential because the D251N mutant exhibits at least a 100-fold decrease in activity.[8] What little activity is left at lower pH exhibits a kinetic solvent isotope effect of about 10 compared to 1.8 for wild-type P450cam.[9] These results indicate that Asp251 is part of an essential proton relay network required for protonation of the iron-linked O_2 molecule, which ensures proper protonation of the distal O atom, thereby resulting in heterolytic cleavage of the O-O bond and formation of Compound I. Although it traditionally has been thought that the closed state must be the active conformer, in the closed state, Asp251 is tied up with salt bridges to Lys178 and Arg186 and thus is not free to shuttle protons to the iron-linked O_2 molecule (Figure 2). However, when Pdx binds, these salt bridges are broken (Figure 2), which frees Asp251 to participate in the required proton relay network: hence, the "Asp switch hypothesis". Supporting this idea is the unexpected observation that in the P450cam-Pdx crystal structure, the product, 5-*exo*-hydroxycamphor, and not camphor is in the active site,[3] whereas in crystal structures of P450cam in the closed form, product has never been observed. This indicates that X-ray generated reducing equivalents can drive camphor hydroxylation in the open state but not the closed state. One problem with this view is that protein-substrate interactions generally thought to be critical for maintaining regio- and stereoselective hydroxylation would be weakened in the open form. Preliminary molecular dynamics studies comparing the open and closed states indeed show that the camphor is much more mobile in the open state, which is incompatible with the strict regio-

and stereoselectivity exhibited by P450cam. We therefore have carried out more extensive MD simulations to determine the effect of Pdx on the conformational space sampled by P450cam and on substrate mobility. In addition, we explore the importance of the Asp251 salt bridge with Arg186 using mutagenesis, steady-state kinetics, product analysis, and crystallography.

EXPERIMENTAL SECTION

Computational Method

Three structures were used for the simulations. The substrate-bound closed structure (5CP4), the P450cam-Pdx structure (4JX1) where P450cam is in the open conformation, and the same P450cam open structure in 4JX1, except Pdx was removed. The maleamide interprotein cross-link used to stabilize the P450cam-Pdx complex was not included in the simulations. In all three, crystallographic waters were retained. Details of the parameters and force field including parameters for the ferric heme used were the same as previously described.[10] Briefly, each structure was solvated in a rectangular box of TIP3 waters with a 10 Å cushion and Na^+ ions in order to maintain net neutrality. Asp297, which is buried in the active site and H-bonds with a heme propionate, was protonated. Each structure was energy minimized for 1000 cycles, allowing only H atoms and solvent molecules to move, and then another 1000 cycles, where all atoms were allowed to move. Production runs were made with Amber14 using the same input parameters as described earlier.[10] The main difference is that 0.002 ps steps were taken rather than 0.001 ps, frames were saved every 20 ps, and Amber 14 rather than Amber 12 was used. Several 100 ns simulations were carried out that differed in the initial random starting velocity. Prior to production runs, backbone CA and camphor atoms were restrained with a 1 kcal/mol force constant for 5 ns followed by 100 ns production runs with no restraints. These simulations were used to compare substrate mobility. Single, longer 500 ns runs also were carried out and used for principal component analyses (PCA). Analyses were performed with ptraj and cpptraj in the AmberTools as well as home-built shell scripts. PCA were similar to those previously described.[6,11] The first step was to generate an average structure of the open and closed conformers. To do this, we used the rigimol program in Pymol (Schrodinger), which is able to morph structures between two conformational states. In our case, 100 structures were generated between the known crystal structures of the open and closed states and a pseudo-Amber MD trajectory file was generated using these 100 structures. The average of these 100 structures then was saved as an Amber coordinate file called *average-structure* to be used as a reference for rms fits. Ptraj or cpptraj were used to generate a covariance matrix of CA atoms by first carrying out an rms fit of the pseudo-MD trajectory to *average-structure* followed by analyzing the resulting matrix and storing the vectors for the first two principal components in a file called *vector-file*. Each 500 ns MD trajectory for the closed, open, and complex then was first rms fit to *average-file* and projected on to *vector-file*. The results were displayed by plotting principal component 1 (PC1) versus principal component 2 (PC2). Some postprocessing of MD trajectories was necessary because Amber requires exactly the same number of atoms for all structures, and the open and closed structures differ by one additional residue at the N-terminus that was not visible in the electron density for the open structure. In addition to this modification and given that we are only interested in

backbone motions, all side chains and H atoms were removed from the MD trajectories. These smaller files contained exactly the same number of atoms and greatly improved the speed of calculations. Production MD runs using Amber 14[12] were carried out using the GPU clusters at the UCSD San Diego Supercomputer Center, whereas analyses were carried out on local linux computers. Active site volume calculations were carried out with voidoo.[13] The internal active site cavity centered on the camphor C5 carbon atom accessible to a 1.4 Å probe was calculated for 15 000 snapshots for P450cam in the closed, open, and complex trajectories.

Protein Expression and Purification

The mutant P450cam, CYP101D1, and their redox partners were expressed and purified from *Escherichia coli* as described previously.[14–17] All UV-visible spectroscopy was performed using a Cary 3 spectrophotometer. P450 content was measured by a reduced CO difference spectrum using an extinction coefficient of 91 mM^{-1} cm^{-1} at 450 nm.[18] Concentrations of Pdx and PdR were determined using extinction coefficient of 5.9 mM^{-1} cm^{-1} at 455 nm and 11.0 $mM^{-1}cm^{-1}$.[19,20] Concentrations of the CYP101D1 redox proteins, Arx and ArR, were calculated using extinction coefficients of 9.3 mM^{-1} cm^{-1} at 414 nm and 10.0 mM^{-1} cm^{-1} at 458 nm, respectively.[19,20] ArR is a flavoprotein that transfers NADH derived electrons to the Fe_2S_2 ferredoxin, Arx, which, in turn, reduces the CYP101D1 heme.

Enzyme Assays

Cytochrome P450 hydroxylation activity was determined in the complete system of three proteins (CYP101D1, ArR, and Arx or P450cam, Pdx, and PdR) by measuring rates of camphor-dependent NADH oxidation at 25 °C following previously established protocols.[21] The concentration of proteins and substrates used ensured that the rates measured were under steady-state saturating conditions. Briefly, the reaction mixture of 1.2 mL contained 0.5 μM ArR/PdR, 5 μM Arx/Pdx, and 0.5 μM P450 in 50 mM Tris (pH 7.4). The rate of NADH oxidation was measured by monitoring the absorbance change at 340 nm using an extinction coefficient of 6.22 mM^{-1} cm^{-1}. The reaction was initiated by first adding NADH (final concentration of 500 μM) in the absence of camphor to obtain the background rate. Substrate-dependent NADH oxidation was then assayed in the presence of 500 μM camphor and was calculated as the difference between the measured rate and the rate of nonspecific NADH oxidation in the absence of camphor (background). After the completion of the reaction (followed by UV/vis), the reaction mixture was subjected to organic extraction with dichloromethylene for product formation analysis using GC-MS according to the previously established protocol.[22]

Crystallography

Crystals of the ferric camphor-bound R186AP450cam mutants were grown at room temperature using the hanging drop vapor diffusion method in 50 mM Tris-HCl buffer, pH 7.4, 400 mM KCl, 32% polyethylene glycol 4000, and 1.2 mM D-camphor as the reservoir solution. The initial droplets containing 2 μL of protein solution at a concentration of 35 mg/mL and 2 μL of the reservoir solution were equilibrated against 500 μL of the reservoir solution. To generate the cyanide complex, the ferric camphor-bound crystals were soaked for 10–15 min at room temperature in ~50 mM buffered potassium cyanide (in 100 mM

Tris-HCl pH 7.4, 400 mM KCl, 32% polyethylene glycol 4000, and 1 mM D-camphor) and then flash-cooled in liquid nitrogen. The brown ferric camphor-bound crystals turned red upon cyanide binding. All data were collected remotely using the Stanford Synchrotron Radiation Lightsource (SSRL) beamline 14-1. Data were indexed, integrated, and scaled with either MOSFLM[23] or XDS.[24] Molecular replacement calculations were conducted with Phaser[25] through the CCP4i[26] graphic interface using ferric camphor-bound wild-type P450cam [Protein Data Bank (PDB) entry 2CPP] as a search model. Further structure refinements were performed using Phenix.refine.[27] Table S1 lists data collection and refinement statistics.

Isothermal Titration Calorimetry (ITC)

All experiments were performed with the MicroCal PEAQ-ITC instrument from Malvern. Phosphate buffer (50 mM at pH 7.4) was used for all experiments. For experiments in the presence of camphor, a final concentration of 1 mM D-camphor was used. DTT or any other reducing agents were removed from both protein preparations before experiments. All experiments were performed at 25 °C. For camphor and Pdx binding experiments, the reaction cell contained either 300 μL of 30 to 60 μM wild-type P450cam or R186A mutant, and the injection syringe was filled with 1 mM D-camphor or 2.4 mM Pdx (for Pdx binding experiment). Each titration experiment was performed by using 18 injections of 2 μL with 4 s duration and a 150 s interval between injections. Reference power of 5, high-feedback mode, and a stirring speed of 750 rpm were used for all experiments. All data were analyzed by using the MicroCal PEAQ-ITC analysis software. To obtain the binding enthalpies, the observed enthalpy values were corrected for the enthalpy of dilution obtained under identical conditions with the sample cell containing buffer alone.

RESULTS

Principal Component Analysis

PCA was carried out for three 500 ns MD simulations of P450cam in the open and closed states and in the P450cam-Pdx complex (Figure 3). As a reference, the location for the closed and open crystal structures and the average of these structures are indicated in Figure 3. As might be expected, the 500 ns MD simulation for the closed structure clusters around the closed crystal structure. The 500 ns MD simulation of the open structure, while centered more toward the open crystal structure, is nevertheless more diffuse, which reflects greater flexibility for the open structure. In sharp contrast, when complexed with Pdx, P450cam clusters more toward the closed state even though both MD simulations of the open form and in the complex start with exactly the same open P450cam conformer. Such clustering of closed and open structures has been observed previously using adaptive molecular dynamics simulations.[11] In addition, it has been possible to crystallographically capture conformers between the two open and closed extremes using tethered substrates that trap the access channel in a partially open state.[28] These results indicate that Pdx favors a conformer between the open and closed extremes. A majority of the larger motions in the open MD simulations are due to open/close motions experienced by the F/G loop. A PCA of the open MD simulation after removing the F/G loop is shown in Figure 3B. Without the F/G loop, the conformational space sampled by the remainder of the structure, while still quite diffuse,

moves closer toward the closed state. Thus, while the F/G loop in the complex moves closer to closed, the remainder of the structure more closely resembles the open form. This is evidenced by an overall rms fit of Cα atoms from the average structures taken from the 500 ns simulations. The rms for closed versus open is 4.2 Å, closed versus complex 4.1 Å, and open versus complex 2.3 Å.

Effect of Pdx on Substrate and the Access Channel

These results indicate that Pdx binding on the proximal side of P450cam results in structural perturbations on the opposite distal side of the molecule (F/G loop region in Figure 2). If so, this could be reflected in less flexibility in the F/G loop region. Calculated thermal B factors thus were compared for P450cam in the presence and absence of Pdx. For these calculations, several MD simulations were merged. For open P450cam, MD simulations from a 456, 500, and four 100 ns separate MD simulations were used for P450cam alone and for P450cam complexed with Pdx 500, 509, 300, and three 100 ns separate MD simulations were used. Figure 4 shows the difference in Cα atom B factors (complex-open). The segment between residues 170–190 (the red segment in Figure 4B) experiences a large increase in thermal motion in the absence of Pdx. The F and G helices and the F/G loop experience the largest motion in the open/close transition and, in the open state, provide a channel for substrate entry. Indeed, in the P450cam-Pdx crystal structure, a second camphor molecule is bound in this access channel.[3] It therefore appears that the binding of Pdx on the proximal surface of P450cam results in a substantial decrease in flexibility in the F/G helical region on the opposite side of the P450.

Effect of Pdx on P450cam and Substrate Dynamics

Figure 5 provides the results from several analyses to determine the effect of Pdx on substrate mobility. The traditional parameter to follow is the distance between the camphor atom that is oxidized, C5, and the heme iron. For these analyses, three 100 ns for the closed state and six 100 ns MD simulations for the open state and in the P450cam-Pdx complex are shown. In Figure 5B, the percent of the total number of snapshots where the C5-Fe distance is ≤4.5 Å relative to other camphor carbon atoms is shown. We note that in all these simulations the substrate can flip over, placing C8 and C9 close to the iron. These poses are incompatible with O_2 binding and thus cannot be considered potentially productive binding modes. As a result, snapshots where C8 and C9 are both within 4.0 Å of the iron were excluded from the calculations. The results in Figure 5B shows that with Pdx bound the camphor more frequently samples a productive orientation compatible with C5 hydroxylation. The calculated thermal motion (Figure 5E) is also lower when Pdx is bound, but not as low as in the closed form.

Another important substrate-protein interaction is the H-bond between Tyr96 and the camphor carbonyl oxygen. Whereas this H-bond does not contribute significantly to the free energy of binding, it does contribute to regioselective hydroxylation.[29] In the closed state, this H-bond never breaks, whereas in the open state, the Tyr96-camphor H-bond rarely forms. However, the presence of Pdx substantially increases the fraction of time the Tyr96-camphor H-bond forms (Figure 5C). It also was important to follow the Asp251-Arg186 ion pair central to the “Asp switch hypothesis” as this ion pair must break to enable the proton-

coupled electron transfer machinery to operate. The Asp251-Arg186 ion pair is very stable in the closed state but rarely forms in either the open state or the complex (Figure 5D). Finally, we followed the distance between Asn59 and Gly189 as a measure of the open and closed states. The distance between these two residues changes from 13 to ~21 Å in the closed to open transition. As shown in Figure 5F, this distance in the complex comes closer to matching the open state than the closed state. Therefore, whereas Pdx stabilizes the F/G helical region as well as camphor mobility, Pdx does not result in a complete closure of the active site. Importantly, the Asp251-Arg186 ion pair does not re-form, thereby enabling Asp251 to participate in the required proton relay network. One further indication that Pdx binding favors sampling conformational states between the two open and closed extremes is active site volume. A 1.4 Å solvent probe was placed at the camphor C5 location and the accessible volume calculated for 15 000 frames for the three 100 ns MD simulations for the closed state and for the six 100 ns simulations for open P450cam and P450cam in the complex with Pdx. The percent of the 15 000 frames with a volume accessible to the probe <100 $Å^3$ is 99% (closed), 25.5% (open), and 48.9% (complex). Pdx thus promotes an active site volume midway between the extremes of open and closed.

Analysis of the Asp251 Salt Bridge Mutants

Central to the Asp switch hypothesis is that the Asp251 salt bridge ion paired with Arg186 must break in order for Asp251 to serve its function in catalysis. If correct, then removal of these salt bridges should not greatly effect activity. Our previous studies with K178G mutant of P40cam showed that the Lys178 and Asp251 H-bond was not crucial for catalysis.[30] Here, we generated the Arg186Ala mutant in P450cam and CYP101D1. CYP101D1 is a very close homologue to P450cam and catalyzes the oxidation of camphor to 5-*exo*-hydroxycamphor at the same rate and with the same catalytic efficiency as P450cam.[17,31] Unlike P450cam, however, CYP101D1 exhibits relaxed redox partner selectivity and can utilize the P450cam redox partner, Pdx, to support catalysis, but P450cam cannot use the CYP101D1 ferredoxin redox partner.[32] The Asp251 homologue in CYP101D1, Asp259, also is essential for activity.[17] In CYP101D1, Asp259 salt bridges with Arg188 exactly the same as the Asp251-Arg186 pair in P450cam, although the homology to Lys178 in CYP101D1 is a Gly. The effect of these mutations on catalysis is summarized in Table 1.

Whereas the mutations do lower k_{cat}, the coupling efficiency remains quite high, indicating that nearly all reducing equivalents derived from NADH are utilized for substrate hydroxylation. The decrease in activity is possibly due to an incomplete low- to high-spin conversion upon substrate binding in the R186A mutant (Figure S1). A higher fraction of low-spin will decrease the redox potential of the heme, thus slowing down the first electron transfer step which is rate-limiting.[33] Compared to converting Asp251 to Asn, which decreases activity 100-fold at low pH,[8] removing the Arg or Lys salt bridge partner has only a modest effect on activity. We also characterized the binding of both substrate and Pdx to the R186A mutant using ITC. The K_D for camphor binding to wild-type P450cam is 1.2 ± 0.4 and 32.2 ± 4 μM for the R186A mutant (Figure S2). Therefore, a “loosening” of the substrate access channel ≈10 Å from the substrate binding site decreases the affinity for camphor. However, the K_D = 22.07 ± μM for Pdx binding to substrate-free R186A mutant is

similar to wild-type P450cam (K_D = 19.4 + 1.23 μM),[6] indicating that binding to Pdx was not affected upon mutation.

Crystal Structures

We next solved the crystal structure of the P450cam Arg186Ala mutant including the complex with CN^-. CN^- has been shown to be a very close mimic of O_2 binding since both induce local changes in protein and solvent structure considered important for the proton relay network required to activate O_2.[34] This then provides a snapshot of an important catalytic intermediate. The mutation causes little change in structure, but there is one important and surprising difference. As shown in Figure 6A, product, 5-*exo*-hydroxy-camphor, is bound at the active site.

There have been many crystal structures of P450cam, but only in the P450cam-Pdx crystal structure was product observed.[3] In addition, wild-type CYP101D1 exhibits about 50% product formation.[17] This means that X-ray generated reducing equivalents are able to drive substrate hydroxylation in the R186A mutant, P450cam-Pdx complex, and CYP101D1. The one feature these all have in common is weakened salt bridge pairing with Asp251. In the P450cam-Pdx complex, there are no salt bridges, whereas in CYP101D1, Asp259 is paired with only Arg188 as the homologue to Lys178 in P450cam is a Gly in CYP101D1. As might be expected, the CN^- complex shows only substrate (Figure 6B) but no product as CN^- blocks the binding of O_2, thereby preventing substrate hydroxylation. An interesting feature of the CN^- complex is the change in local solvent structure relative to the unliganded structure. The binding of O_2 or CN^- results in a widening of the I helix that contains Thr252, which enables water to move into the active site to form a potential proton delivery network required for O_2 activation. The CN^- complex of the Arg186Ala mutant shows additional solvent between Asp251 and Asp182 that provides a continuous H-bonded network to bulk solvent. This could thus represent a snapshot of the H-bonding network required for O_2 activation after the Asp251-Arg186 ion pair is broken. For Asp251 to shuttle protons toward the iron-linked O_2 molecule, Asp251 would need to rotate ≈180°. Quite interestingly, Thr252 occupies two orientations. In one of these orientations, there could potentially be a continuous H-bonded link between the iron-linked O_2 molecule, Thr252, and Asp251 if Asp251 is able to adopt another rotamer.

We also carried out five 100 ns MD simulations of the R186A mutant and analyzed the trajectories similar to that shown in Figure 5. As shown in Figure S4, the camphor B factor remains low and the Tyr96-camphor H-bond remains intact, similar to the wild-type closed MD simulations. However, the C5-Fe distance variation more closely resembles the P450cam-Pdx complex. This is consistent with the ITC result,s wherein the affinity for camphor decreases, but apparently, this does not prevent regio- and stereoselective hydroxylation.

CONCLUSIONS

The purpose of this study was to determine if Pdx binding to the open form of P450cam helps to stabilize the active site pocket. This is important because, in the crystal structures of the P450cam-Pdx complex, P450cam is in the open conformation, yet we observe highly

ordered correct product, 5-*exo*-hydroxycamphor, in the active site,[3] which indicates that the substrate must be quite stable in the P450cam-Pdx complex. Because P450cam is open in the P450cam-Pdx crystal structure, this raises the possibility that Pdx binding might be able to help stabilize the active site even though P450cam is in the open conformation. Our simulations indicate that, indeed, Pdx stabilizes the active site and favors conformational states between the two extremes of open and closed. The F/G helical region moves closer to the closed state, but the rms of Cα atoms shows that much of the rest of the structure remains more open. These observations also are consistent with the available crystal structures. There are two crystal structures of the P450cam-Pdx complex. As noted, our structure[3] shows highly ordered product in the active site, and all parts of the active site are well-ordered. The P450cam-Pdx structure of Hiruma et al.[2] also shows P450cam in the open conformation, but glycerol, not camphor, is in the active site and part of the active site B′ helix that provides important substrate contacts is disordered. In the open form, crystal structure of camphor-free P450cam without Pdx bound, the B′ helix region also is disordered.[28] When camphor is bound to this open form, the camphor is not well-ordered and does not bind in a productive orientation.[35] These crystal structures are consistent with our MD simulations: only when both camphor and Pdx are bound is the B′ and F/G helical regions ordered sufficiently to be observed in electron density maps.

The effects of Pdx binding are long-range as Pdx binding to the proximal face of P450cam influences the dynamics on the opposite side of the protein. The open/close motion of the F/G helical region is coupled to movement of the C helix, which directly contacts Pdx (Figure 2). Most importantly, Pdx-induced changes in the F/G helical region which frees Asp251 to serve its role in the proton delivery network required for O_2 activation. Our MD simulations also show that even though Pdx stabilizes the active site and F/G helical region, Asp251 rarely re-forms an ion pair with Arg186 and thus remains free to serve its catalytic role. These results indicate that Arg186 may not be very important for catalysis. This view is consistent with our finding that the R186A mutant retains substantial activity. Moreover, like CYP101D1 and the P450cam-Pdx complex, X-ray generated reducing equivalents drive substrate hydroxylation in the Arg186Ala mutant, further supporting the view that weakened ion pairing interactions with Asp251 are important for O_2 activation.

Finally, we note that very similar open/close motions have been crystallographically observed in other P450s, wherein movement of the F/G helical region is coupled to movement of the C helix that contacts the redox partner.[36] It therefore may be a general property of P450s that structural changes at the redox partner binding site are coupled to changes in the substrate access channel and, possibly, stabilization of the substrate binding pocket. It remains to be seen, however, if the extreme selectivity of P450cam for its redox partner and the effector role of Pdx is exhibited in other P450s.

Supplementary Material

Refer to Web version on PubMed Central for supplementary material.

Acknowledgments

This work was supported by NIH Grant GM57353. We wish to thank the SSRL and ALS beamline staff for their support during remote X-ray diffraction data collection. We also thank Alec Follmer for reading the manuscript and helpful suggestions.

References

1. Lipscomb JD, Sligar SG, Namtvedt MJ, Gunsalus IC. J Biol Chem. 1976; 251:1116. [PubMed: 2601]
2. Hiruma Y, Hass MA, Kikui Y, Liu WM, Olmez B, Skinner SP, Blok A, Kloosterman A, Koteishi H, Lohr F, Schwalbe H, Nojiri M, Ubbink M. J Mol Biol. 2013; 425:4353. [PubMed: 23856620]
3. Tripathi S, Li H, Poulos TL. Science. 2013; 340:1227. [PubMed: 23744947]
4. Myers WK, Lee YT, Britt RD, Goodin DB. J Am Chem Soc. 2013; 135:11732. [PubMed: 23901883]
5. Unno M, Christian JF, Benson DE, Gerber NC, Sligar SG, Champion PM. J Am Chem Soc. 1997; 119:6614.
6. Hollingsworth SA, Batabyal D, Nguyen BD, Poulos TL. Proc Natl Acad Sci U S A. 2016; 113:8723. [PubMed: 27439869]
7. Pochapsky SS, Pochapsky TC, Wei JW. Biochemistry. 2003; 42:5649. [PubMed: 12741821]
8. Gerber NC, Sligar SG. J Biol Chem. 1994; 269:4260. [PubMed: 8307990]
9. Vidakovic M, Sligar SG, Li H, Poulos TL. Biochemistry. 1998; 37:9211. [PubMed: 9649301]
10. Hollingsworth SA, Poulos TL. Protein Sci. 2015; 24:49. [PubMed: 25307478]
11. Markwick PR, Pierce LC, Goodin DB, McCammon JA. J Phys Chem Lett. 2011; 2:158. [PubMed: 21307966]
12. Salomon-Ferrer R, Goetz AW, Poole D, Le Grand S, Walker RC. J Chem Theory Comput. 2013; 9:3878. [PubMed: 26592383]
13. Kleywegt GJ, Jones TA. Acta Crystallogr, Sect D: Biol Crystallogr. 1994; 50:178. [PubMed: 15299456]
14. Sevrioukova IF, Garcia C, Li H, Bhaskar B, Poulos TL. J Mol Biol. 2003; 333:377. [PubMed: 14529624]
15. Sevrioukova IF, Li H, Poulos TL. J Mol Biol. 2004; 336:889. [PubMed: 15095867]
16. Yoshioka S, Takahashi S, Ishimori K, Morishima I. J Inorg Biochem. 2000; 81:141. [PubMed: 11051559]
17. Batabyal D, Poulos TL. Biochemistry. 2013; 52:8898. [PubMed: 24261604]
18. Omura T, Sato R. J Biol Chem. 1964; 239:2370. [PubMed: 14209971]
19. Kuznetsov VY, Blair E, Farmer PJ, Poulos TL, Pifferitti A, Sevrioukova IF. J Biol Chem. 2005; 280:16135. [PubMed: 15716266]
20. Gunsalus IC, Wagner GC. Methods Enzymol. 1978; 52:166. [PubMed: 672627]
21. Sevrioukova IF, Hazzard JT, Tollin G, Poulos TL. Biochemistry. 2001; 40:10592. [PubMed: 11524002]
22. Churbanova IY, Poulos TL, Sevrioukova IF. Biochemistry. 2010; 49:58. [PubMed: 19954240]
23. Battye TG, Kontogiannis L, Johnson O, Powell HR, Leslie AG. Acta Crystallogr, Sect D: Biol Crystallogr. 2011; 67:271. [PubMed: 21460445]
24. Kabsch W. Acta Crystallogr, Sect D: Biol Crystallogr. 2010; 66:125. [PubMed: 20124692]
25. McCoy AJ, Grosse-Kunstleve RW, Adams PD, Winn MD, Storoni LC, Read RJ. J Appl Crystallogr. 2007; 40:658. [PubMed: 19461840]
26. Winn MD, Ballard CC, Cowtan KD, Dodson EJ, Emsley P, Evans PR, Keegan RM, Krissinel EB, Leslie AG, McCoy A, McNicholas SJ, Murshudov GN, Pannu NS, Potterton EA, Powell HR, Read RJ, Vagin A, Wilson KS. Acta Crystallogr, Sect D: Biol Crystallogr. 2011; 67:235. [PubMed: 21460441]

27. Adams PD, Afonine PV, Bunkoczi G, Chen VB, Davis IW, Echols N, Headd JJ, Hung LW, Kapral GJ, Grosse-Kunstleve RW, McCoy AJ, Moriarty NW, Oeffner R, Read RJ, Richardson DC, Richardson JS, Terwilliger TC, Zwart PH. Acta Crystallogr, Sect D: Biol Crystallogr. 2010; 66:213. [PubMed: 20124702]
28. Lee YT, Wilson RF, Rupniewski I, Goodin DB. Biochemistry. 2010; 49:3412. [PubMed: 20297780]
29. Atkins WM, Sligar SG. J Biol Chem. 1988; 263:18842. [PubMed: 3198602]
30. Batabyal D, Li H, Poulos TL. Biochemistry. 2013; 52:5396. [PubMed: 23865948]
31. Yang W, Bell SG, Wang H, Zhou W, Hoskins N, Dale A, Bartlam M, Wong LL, Rao Z. J Biol Chem. 2010; 285:27372. [PubMed: 20576606]
32. Batabyal D, Lewis-Ballester A, Yeh SR, Poulos TL. Biochemistry. 2016; 55:6517. [PubMed: 27808504]
33. Kuznetsov VY, Poulos TL, Sevrioukova IF. Biochemistry. 2006; 45:11934. [PubMed: 17002293]
34. Fedorov R, Ghosh DK, Schlichting I. Arch Biochem Biophys. 2003; 409:25. [PubMed: 12464241]
35. Liou SH, Mahomed M, Lee YT, Goodin DB. J Am Chem Soc. 2016; 138:10163. [PubMed: 27452076]
36. Poulos TL. Chem Rev. 2014; 114:3919. [PubMed: 24400737]

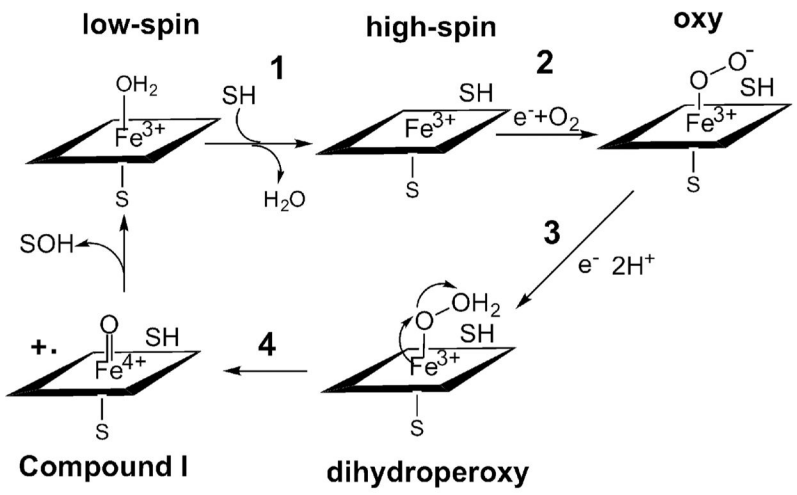

Figure 1.

P450 catalytic cycle. After substrate binding (step 1), electron transfer from a redox partner (step 2) reduces the heme iron, which enables O_2 to bind. A second proton-coupled electron transfer (step 3) forms the transient dihydroperoxy intermediate. After heterolytic cleavage of the O-O bond (step 4), Compound I is formed followed by substrate hydroxylation.

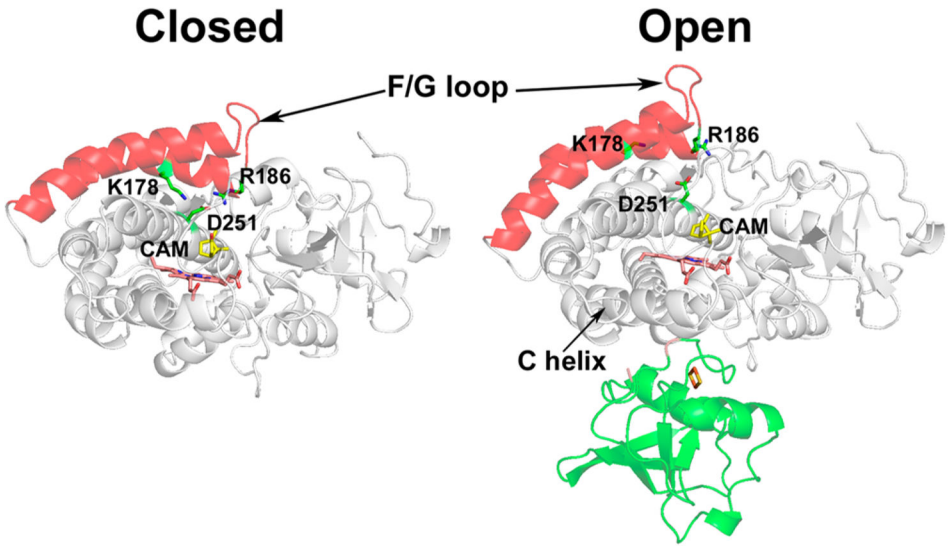

Figure 2.

Comparison of the P450cam closed (5CP4) and the open state in complex with Pdx (4JX1). The F and G helices are colored red. In the closed state, Asp251 is ion paired with Lys178 and Arg186. In the open state in the complex with Pdx, the F helix and F/G loop undergo a large change that opens up the active site, resulting in a rupture of the Asp251 ion pairs. Asp251 now is free to serve its role in proton transfer to the iron-linked dioxygen.

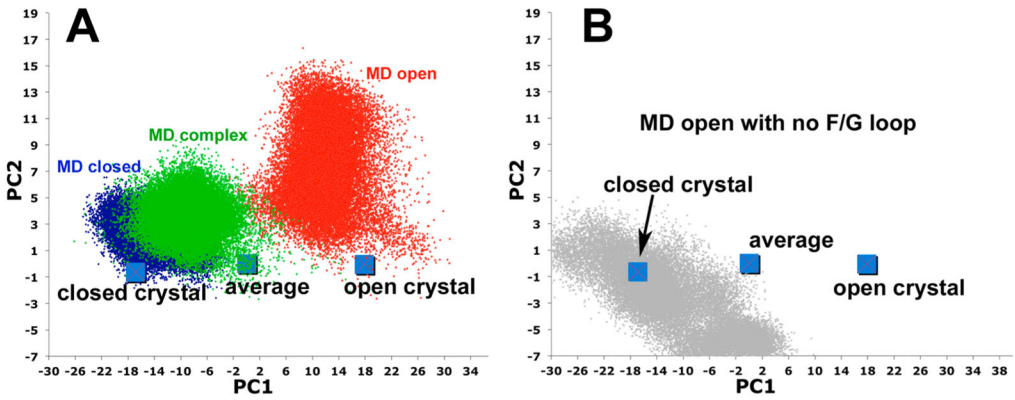

Figure 3.

PCA of P450cam in the closed (blue) and open (red) conformers and P450cam in a complex with Pdx (green). The only difference between the starting structures for the open form and in the Pdx complex is the presence or absence of Pdx. Each simulation is for 500 ns. As shown in panel A, the presence of Pdx shifts P450cam more toward the closed form even though the simulations start closer to the open crystal structure. Panel B shows the effect of removing the F/G loop Pdx-free open structure. The open form now clusters more toward the closed crystal structure, which illustrates that the dynamics of the F/G loop and F helix contribute most to the various conformational states.

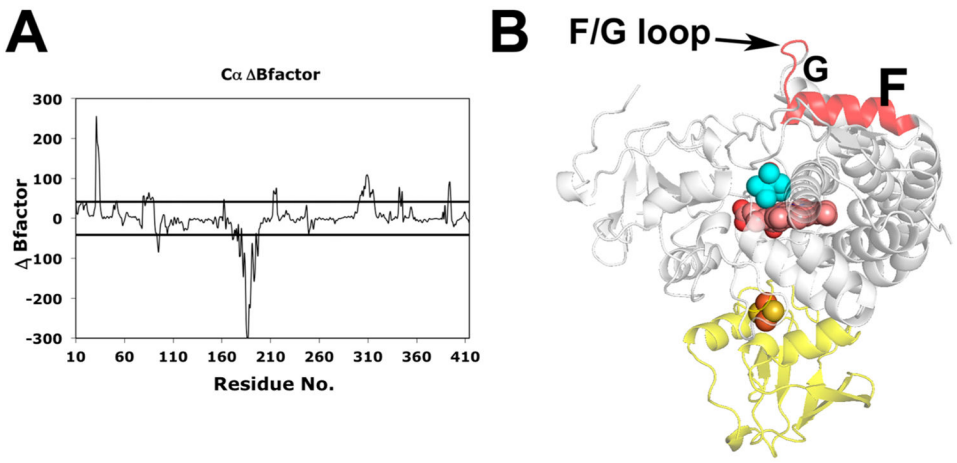

Figure 4.

ΔB factor plot (complex-open) as a function of residue number. For the open state MD trajectories runs of 456, 500, and four 100 ns were merged, whereas for P450cam in the complex runs of 500, 509, 300, and three 100 ns were merged. Merging several runs in this way reduced the standard deviations, which are represented as solid lines in panel A. Pdx binding substantially decreases the B factors of the F/G loop and F helix region (red segment in panel B).

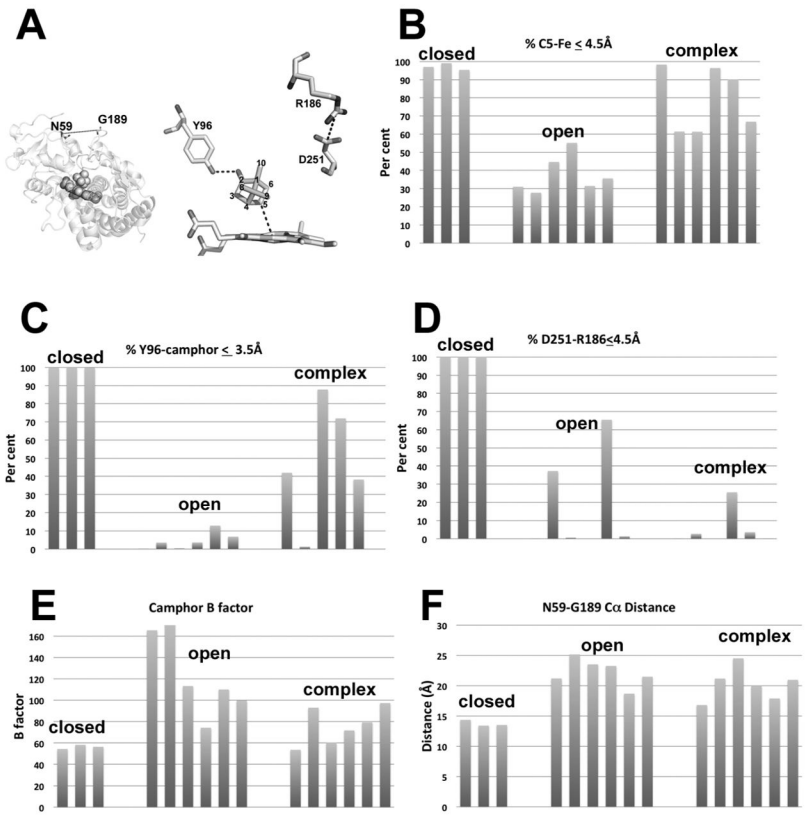

Figure 5.

Results of distance and B factor analyses for three 100 ns runs for closed P450cam and six 100 ns runs each for open P450cam and P450cam complexed with Pdx. There are 0.02 ns per snapshots, giving a total of 5000 snapshots per MD trajectory. (A) Models illustrating the various distances used for the analyses. (B) Percent of snapshots where the camphor C5-Fe distance is ≤4.5 Å relative to other camphor C atoms; (C) percent of snapshots where the Tyr96-camphor carbonyl O atom distance is ≤3.5 Å; (D) percent of snapshots where the Asp251 CG-Arg186 NZ distance is <4.5 Å; (E) calculated B factor for camphor; (f) distance between CA atoms of Asn59 and Gly189.

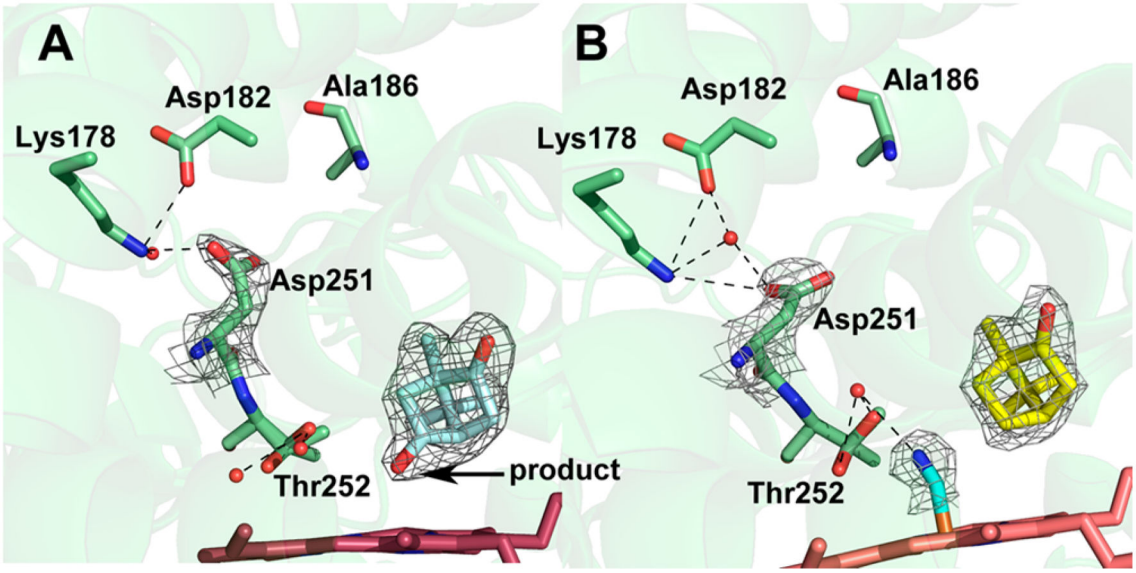

Figure 6.

$2F_o$-F_c electron density maps of the P450cam Arg186Ala mutant contoured at 1.0 σ. (A) With no ligand, 5-*exo*-hydroxycamphor is bound at the active site, indicating that X-ray generated reducing equivalents drive substrate hydroxylation. (B) CN^- complex showing substrate, but no product is bound. In both structures, Thr252 adopts two orientations.

Table 1

Enzyme Activity and Coupling Efficiency of Wild Type and Salt Bridge Mutants

P450 type	NADH turnover (min^{-1})	coupling efficiency[a] (%)	ref
WT P450cam	930 ± 28	95	this work
K178G P450cam	395 ± 20	91	27
R186AP450cam	288 ± 10	75	this work
WTCYP101D1	950 ± 30	96	15
R188ACYP101D1	210 ± 8	74	this work

[a]Coupling efficiency is the % NADH used to produce one product molecule. In a 100% coupled P450, 1.0 product equivalents is produced per 1.0 NADH consumed.